Original Article

Regional variation in paraspinal muscle composition using chemical shift encoding-based water-fat MRI

Nico Sollmann[1], Agnes Zoffl[1], Daniela Franz[2], Jan Syväri[2], Michael Dieckmeyer[1], Egon Burian[1], Elisabeth Klupp[1], Dennis M. Hedderich[1], Christina Holzapfel[3], Theresa Drabsch[3], Jan S. Kirschke[1], Ernst J. Rummeny[2], Claus Zimmer[1], Hans Hauner[3], Dimitrios C. Karampinos[2], Thomas Baum[1]

[1]Department of Diagnostic and Interventional Neuroradiology, [2]Department of Diagnostic and Interventional Radiology, [3]Institute for Nutritional Medicine, Klinikum rechts der Isar, Technische Universität München, Munich, Germany

Correspondence to: Nico Sollmann, MD, PhD. Department of Diagnostic and Interventional Neuroradiology, Klinikum rechts der Isar, Technische Universität München, Ismaninger Str. 22, 81675 Munich, Germany. Email: Nico.Sollmann@tum.de.

Background: Paraspinal musculature forms one of the largest muscle compartments of the human body, but evidence for regional variation of its composition and dependency on gender or body mass index (BMI) is scarce.

Methods: This study applied six-echo chemical shift encoding-based water-fat magnetic resonance imaging (MRI) at 3 Tesla in 76 subjects (24 males and 52 females, age: 40.0±13.7 years, BMI: 25.4±5.6 kg/m²) to evaluate the proton density fat fraction (PDFF) of psoas muscles and erector spinae muscles, with the latter being divided into three segments in relation to levels of spine anatomy (L3–L5, T12–L2, and T9–T11).

Results: For the psoas muscles and the erector spinae muscles (L3–L5), gender differences in PDFF values were observed (PDFF psoas muscles: males: 5.1%±3.4% *vs.* females: 6.0%±2.2%, P=0.006; PDFF erector spinae muscles L3–L5: males: 10.7%±7.6% *vs.* females: 18.2%±6.8%, P<0.001). Furthermore, the PDFF of the erector spinae muscles (L3–L5) showed higher PDFF values when compared to the other segments (PDFF erector spinae muscles L3–L5 *vs.* T12–L2: P<0.001; PDFF erector spinae muscles L3–L5 *vs.* T9–T11: P<0.001) and showed to be independent of BMI, which was not the case for the other segments (T12–L2 or T9–T11) or the psoas muscles. When considering age and BMI as control variables, correlations of PDFF between segments of the erector spinae muscles remained significant for both genders.

Conclusions: This study explored regional variation of paraspinal muscle composition and dependency on gender and BMI, thus offering new insights into muscle physiology. The PDFF of the erector spinae muscles (L3–L5) was independent of BMI, suggesting that this level may be suited for representative paraspinal muscle segmentation and PDFF extraction as a biomarker for muscle alterations in the future.

Keywords: Muscular fat deposition; paraspinal musculature; proton density fat fraction (PDFF); quantitative imaging; spine

Submitted Aug 07, 2019. Accepted for publication Jan 09, 2020.
doi: 10.21037/qims.2020.01.10
View this article at: http://dx.doi.org/10.21037/qims.2020.01.10

Introduction

Several factors have been shown to lead to a positive energy balance, with aging, consumption of high caloric food or drinks, and lack of physical exercise being among the most prominent ones (1-3). A dysregulation of energy homeostasis can result in adiposity that is characterized by an accretion of fat in different tissues of the human body, with subcutaneous fat accumulation representing the major physiological buffer (4-6). However, the storage capacity of subcutaneous tissue is limited; therefore, when its capacity is exceeded and its expandability is restricted,

fat may also accumulate in other tissues (4-6). Against this background, muscular tissue can serve as an ectopic fat store, thus being able of absorbing fat. In the past, several studies have investigated elevated muscular fat fractions, particularly in the course of various metabolic, neuromuscular, degenerative or other diseases (7-16). Of note, the paraspinal musculature makes up one of the largest muscle compartments of the human body, but has rarely been studied when exploring characteristics of ectopic fat deposition.

Fat composition of the human body can be assessed in-vivo using different imaging techniques. Dual energy X-ray absorptiometry (DXA), computed tomography (CT), and magnetic resonance imaging (MRI) are the most broadly used techniques to date (17-19). DXA is able to discriminate between bony structures, fat, and lean soft tissue, whereas CT can also determine adipose tissue volumes and the amount of fat deposition (17-20). MRI principally allows for both qualitative and quantitative evaluation of fat composition without radiation exposure and enables the evaluation of more sophisticated parameters, including assessments of specific regional fat distributions and fat phenotyping, for instance (17-19,21). However, most previous MRI-based studies applied conventional T1-weighted or T2-weighted sequences, thus primarily enabling qualitative analyses of fat composition. Quantitative, more objective assessments of fat composition become possible when using advanced MRI techniques, such as chemical shift encoding-based water-fat MRI that has proven to be a time-efficient, field map-insensitive, and accurate technique enabling spatially resolved fat quantification (17-19,21-24). In chemical shift encoding-based water-fat MRI, determination of the proton density fat fraction (PDFF) as a parameter representing the fat fraction is a reliable approach to obtain quantitative values on the fat composition of different body compartments or areas, with good concordance between such PDFF measurements and histologic findings or magnetic resonance spectroscopy (MRS) as the gold-standard method (22,25-29). When combined with conventionally used assessments of the cross sectional area (CSA), one can obtain information on both morphological sizes as well as fat fractions of specific muscles.

Although paraspinal musculature is one of the largest muscle compartments of the human body, its potential regional variation and dependency of region-specific fat fractions on gender or body mass index (BMI) are largely unknown to date. However, elucidating associations of fat fractions derived from paraspinal musculature may offer novel insight into basal muscle physiology and could further contribute to our understanding of diseases that entail alterations in fat composition and distribution. This plays a role given the close spatial and functional interactions of the paraspinal musculature and the adjacent vertebral column that is responsible for fundamental characteristics like body movement, spine stabilization, or balance keeping (30,31). Against this background, the purpose of this study was to systematically investigate potential regional variation in paraspinal muscle fat composition and distribution, depending on gender and BMI, using evaluations of the PDFF and CSA as derived from chemical shift encoding-based water-fat MRI.

Methods

Ethics

This study was approved by the Institutional Review Board (registration number: 2719/10 S) and was conducted in accordance with the Declaration of Helsinki. Written informed consent was obtained from all study participants.

Study cohort

Subjects investigated were part of a large study aiming at exploring determinants of basal metabolic rate and were recruited at the Institute for Nutritional Medicine, Klinikum rechts der Isar, Technical University of Munich. Out of the various assessments performed for the investigation, the present study focusses on parameters derived from imaging by chemical shift encoding-based water-fat MRI to explore regional variation in paraspinal muscle fat composition and distribution, depending on gender and BMI. The study included volunteers who were at least 18 years old and had a BMI larger or equal to 18.5 kg/m^2. In this context, the individual BMI was calculated as the quotient of weight (in kg) and height (in m) squared (kg/m^2). Subjects who had any history of severe diseases or surgery within the last three months, had acute physical impairment, or were pregnant or breast-feeding were excluded.

Overall, 111 volunteers were initially recruited for the investigation of determinants of basal metabolic rate, 76 of these volunteers were considered in the present study. Thirty-two volunteers did not provide consent for the imaging part of the investigation or had contraindications for MRI and, thus, did not undergo imaging by chemical

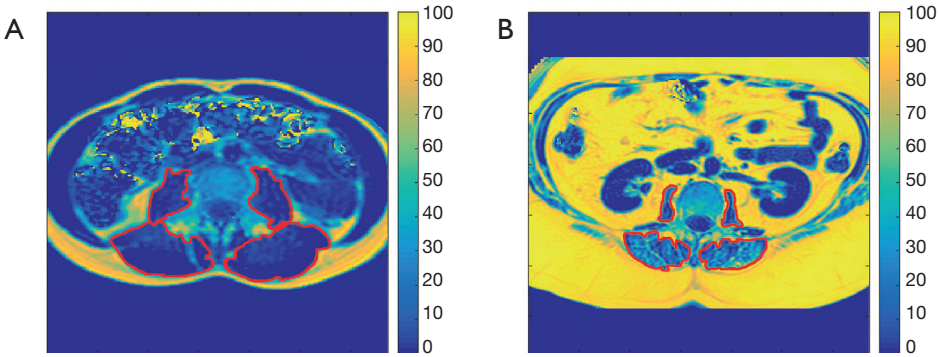

Figure 1 Proton density fat fraction (PDFF) maps. Representative axial PDFF maps of a 27-year-old female with a body mass index (BMI) of 20.5 kg/m^2 at the level of L4 (A) and a 38-year-old male with a BMI of 37.6 kg/m^2 at the level of L3 (B). Color coding was applied to these maps according to PDFF values (in %), ranging from dark blue to bright yellow. The bilateral psoas and erector spinae muscles are schematically enclosed by red contours.

shift encoding-based water-fat MRI. Another three subjects were excluded due to artifacts in imaging data or a field of view (FOV) that was too small, leading to a final cohort size of 76 subjects being considered in the present study (mean age: 40.0±13.7 years, age range: 21.2–77.3 years, median age: 38.0 years).

MRI

Subjects underwent MRI at 3 Tesla (Ingenia, Philips Healthcare, Best, Netherlands) using a six-echo multi-echo gradient echo sequence for chemical shift encoding-based water-fat separation. Scanning was performed in supine position using anterior and posterior coil arrays.

The entire abdomen was covered by two axial stacks using the following sequence parameters per stack: TR/TE1/ΔTE =7.8/1.35/1.1 ms, FOV =300×400×150 mm^3, fold-over suppression in both L/R directions with 50 mm, acquisition matrix size =152×133, acquisition voxel size =2×3×6 mm^3, sensitivity encoding (SENSE) with reduction factor =2.2×1.2, receiver bandwidth =1,678 Hz/pixel, frequency direction =A/P (to minimize breathing artifacts), acquisition during a breathhold duration of 15 s per stack. The sequence acquired the six echoes in a single TR using bipolar readout gradients and applied a flip angle of 3° to reduce T1 bias effects (24,32-34).

Fat quantification

For fat quantification, the MRI data were first processed using the vendor's routines. In this context, phase error correction and a complex-based water-fat decomposition considering a pre-calibrated seven-peak fat spectrum and a single T2* were applied (mDIXON, Philips Healthcare, Best, Netherlands). PDFF maps were computed as the ratio of the fat signal over the sum of fat and water signals (*Figure 1*).

Extraction of PDFF and CSA

Regions of interest (ROIs) were manually drawn in the PDFF maps of each subject using MITK [http://mitk.org/wiki/The_Medical_Imaging_Interaction_Toolkit (MITK); German Cancer Research Center, Division of Medical and Biological Informatics, Medical Imaging Interaction Toolkit, Heidelberg, Germany]. The right erector spinae muscle, left erector spinae muscle, right psoas muscle, and left psoas muscle were identified and carefully enclosed by muscle-specific ROIs on each axial slice showing these muscles (*Figure 2*). All ROIs were placed at the muscle contour whilst avoiding the inclusion of subcutaneous fat or the muscle-fat interfaces (*Figure 2*).

Subsequent to ROI placements, we extracted the PDFF (in %) and CSA (in cm²) for each subject and muscle by averaging the respective values derived from the muscle-specific ROIs placed in the consecutive axial slices. For the right and left erector spinae muscles, we defined three segments that were analyzed separately, which were determined according to anatomical localization in relation to thoraco-lumbar spine anatomy. These three segments covered the right and left erector spinae muscles from the lower endplate level of L5 to the upper endplate level of L3, the lower endplate level of L2 to the upper endplate

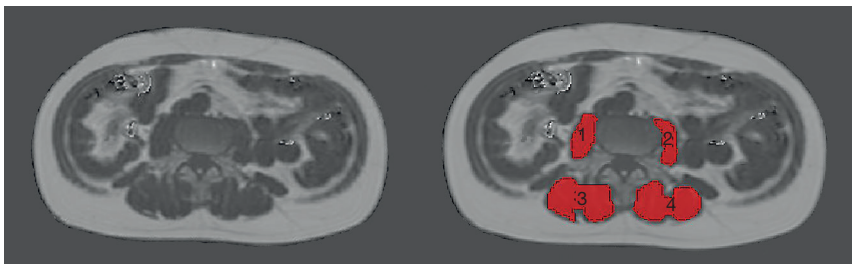

Figure 2 Muscle segmentations. Representative illustration of the placement of regions of interest (ROIs) in axial proton density fat fraction (PDFF) maps in a 53-year-old male with a body mass index (BMI) of 20.7 kg/m^2. The ROIs spatially enclosed the right psoas muscle [1], left psoas muscle [2], right erector spinae muscle [3], and left erector spinae muscle [4].

level of T12, and the lower endplate level of T11 to the upper endplate level of T9. The separation into the three segments was not based on physiological considerations, but aimed at a balanced split of the lower thoracic and lumbar spine. The values obtained for both sides were averaged, leading to one PDFF and CSA value for the psoas muscles and three segment-wise PDFF and CSA values for the erector spinae muscles per subject.

Placement of ROIs was performed by the same reader in all subjects (MD with experience in radiological imaging since 2012). To assess inter-reader reproducibility, a second reader (MD with experience in radiological imaging since 2017) segmented five randomly selected subjects again, being blinded to the ROIs of the first reader. The same approach of ROI placements was followed by both readers.

Statistical analyses

SPSS (version 20.0; IBM SPSS Statistics for Windows, Armonk, NY, USA) and GraphPad Prism (version 6.04; GraphPad Software Inc., La Jolla, CA, USA) were used for statistical analyses. For statistical tests, the level of significance was set at $P<0.05$ (two-sided).

Descriptive statistics including absolute frequencies for categorical variables and mean ± standard deviation for continuous variables were calculated. The Kolmogorov-Smirnov test indicated non-normal distribution for the majority of data. We performed Mann-Whitney U tests to compare age, BMI, PDFF, CSA, and CSA/BMI of the psoas muscles and the three segments of the erector spinae muscles between male and female subjects as well as between subjects younger and older than 38 years (median age of the cohort: 38.0 years), respectively. Furthermore, we performed Wilcoxon signed-rank tests to compare the PDFF of the psoas muscles and the three segments of the erector spinae muscles against each other, respectively. Regarding analysis of reproducibility, we calculated the root mean square coefficient of variation in percent (relative units) based on the PDFF measurements for those datasets that were evaluated by two readers (35).

Correlation analyses using Spearman's rho were carried out considering age, BMI, PDFF of the psoas muscles and the three segments of the erector spinae muscles, followed by partial correlation analyses stratified by gender and using age and BMI as control variables. Bonferroni correction for multiple testing was applied for all correlation analyses.

Results

Cohort characteristics

We included 76 subjects (24 males and 52 females), with PDFF and CSA values of the psoas muscles and the three segments of the erector spinae muscles being available from all subjects. There were no significant differences in age (males: mean age: 39.5±10.5 years, age range: 26.9–61.3 years; females: mean age: 40.3±14.9 years, age range: 21.2–77.2 years; $P=0.733$) or BMI (males: mean BMI: 27.0±5.8 kg/m^2, BMI range: 20.1–41.3 kg/m^2; females: mean BMI: 24.6±5.3 kg/m^2, BMI range: 17.2–43.5 kg/m^2; $P=0.067$) between genders.

Measurements of PDFF and CSA

When considering the PDFF measurements of the three segments of the erector spinae muscles there was a regional variation depending on the anatomical localization. The PDFF of the erector spinae muscles of the segment L3–L5 showed the highest values when compared to the corresponding measurements of the segments T12–L2 and T9–T11 for

Table 1 Mean values ± standard deviation of the proton density fat fraction (PDFF, in %) and cross-sectional area (CSA, in cm^2) of the erector spinae muscles of the segments L3–L5, T12–L2, and T9–T11 as well as the psoas muscles for male and female subjects, respectively. Furthermore, the CSA divided by the body mass index (BMI, in kg/m^2) is provided

Variable	Value	Males (n=24)	Females (n=52)	P
Erector spinae muscles L3–L5	PDFF (in %)	10.7±7.6	18.2±6.8	<0.001
	CSA (in cm^2)	229.5±41.6	179.0±27.7	<0.001
	CSA/BMI	8.6±1.3	7.4±1.3	<0.001
Erector spinae muscles T12–L2	PDFF (in %)	6.1±4.9	7.0±4.5	>0.05
	CSA (in cm^2)	206.0±45.4	142.1±26.5	<0.001
	CSA/BMI	7.9±2.5	5.9±1.1	<0.001
Erector spinae muscles T9–T11	PDFF (in %)	7.1±6.2	6.8±5.0	>0.05
	CSA (in cm^2)	115.7±25.6	79.7±14.4	<0.001
	CSA/BMI	4.4±1.4	3.4±0.8	0.002
Psoas muscles	PDFF (in %)	5.1±3.4	6.0±2.2	0.006
	CSA (in cm^2)	140.7±32.6	94.5±16.8	<0.001
	CSA/BMI	5.5±1.9	4.0±1.0	<0.001

both genders (*Table 1*). Accordingly, there was a significant difference between PDFF values of the segment L3–L5 and the PDFF values of the segments T12–L2 (P<0.001) and T9–T11 (P<0.001), whereas the difference between the PDFF values of the segment T12–L2 and T9–T11 did not show significance (P=0.959). Furthermore, a significant difference was present when comparing the PDFF of the psoas muscles to the measurements derived from the erector spinae muscles of the segments L3–L5 (P<0.001) and T12–L2 (P=0.022), but not for the segment T9–T11 (P=0.073).

Compared to females, males showed significantly lower PDFF values for the psoas muscles (P=0.006) and erector spinae muscles of the segment L3–L5 (P<0.001), in contrast to the segments T12–L2 (P=0.269) or T9–T11 (P=0.947; *Table 1*). CSA values were significantly higher in males when compared to females for the psoas muscles and all segments of the erector spinae muscles (P<0.001; *Table 1*).

Compared to subjects older than 38 years, young subjects showed significantly lower PDFF values for the psoas muscles and erector spinae muscles of the segment L3–L5, T12–L2, and T9–T11 (P<0.001; *Table 2*). CSA values did not show any significant differences in the comparison between subjects older and younger than 38 years (P>0.05; *Table 2*).

Correlations of PDFF between muscles and segments

There were significant correlations among the PDFF of the psoas muscles and the PDFF of all three segments of the erector spinae muscles (P<0.001 for each correlation; *Table 3*). For age, significant correlations with the PDFF of the psoas muscles as well as the PDFF of the three segments of the erector spinae muscles were revealed (P<0.001 for each correlation; *Table 3*). Regarding BMI, significant associations were observed with the PDFF of the psoas muscles (P=0.003) as well as the PDFF of the erector spinae muscles of the segments T12–L2 (P<0.001) and T9–T11 (P<0.001), whereas the association with the PDFF of the segment L3–L5 did not show significance (P=0.495; *Table 3*; *Figure 3*).

When performing partial correlation analyses in males using age and BMI as control variables, significant associations between the PDFF of the different muscles or segments were maintained except for the PDFF of the psoas muscles and the PDFF values of the erector spinae muscles of the segment T9–T11 and for the PDFF values of the erector spinae muscles of the segment L3–L5 and T9–T11 (*Table 4*). In females, significant associations between the PDFF of the different muscles and segments were kept in the partial correlation analyses except for the PDFF values of the erector spinae muscles of the segment L3–L5 and T9–T11 (*Table 5*).

Reproducibility measurements

The reproducibility error expressed as root mean square

Table 2 Mean values ± standard deviation of the proton density fat fraction (PDFF, in %) and cross-sectional area (CSA, in cm^2) of the erector spinae muscles of the segments L3–L5, T12–L2, and T9–T11 as well as the psoas muscles for subjects younger and older than 38 years, respectively. Furthermore, the CSA divided by the body mass index (BMI, in kg/m^2) is provided

Variable	Value	Age <38 years (n=38)	Age >38 years (n=38)	P
Erector spinae muscles L3–L5	PDFF (in %)	12.3±5.6	19.4±8.2	<0.001
	CSA (in cm^2)	191.6±41.3	198.3±38.9	>0.05
	CSA/BMI	8.2±1.4	7.4±1.4	0.015
Erector spinae muscles T12–L2	PDFF (in %)	4.2±2.5	9.2±5.0	<0.001
	CSA (in cm^2)	159.9±52.5	164.6±35.5	>0.05
	CSA/BMI	6.8±2.3	6.2±1.5	>0.05
Erector spinae muscles T9–T11	PDFF (in %)	4.1±2.7	9.6±6.0	<0.001
	CSA (in cm^2)	94.5±27.8	87.6±21.4	>0.05
	CSA/BMI	4.0±1.1	3.4±1.1	0.008
Psoas muscles	PDFF (in %)	4.5±1.5	6.9±2.9	<0.001
	CSA (in cm^2)	115.1±34.7	103.1±26.6	>0.05
	CSA/BMI	4.9±1.6	3.9±1.2	0.002

Table 3 Whole-group correlation analyses using Spearman's rho and considering the variables age, body mass index (BMI), proton density fat fraction (PDFF) of the erector spinae muscles of the segments L3–L5, T12–L2, and T9–T11, and PDFF of psoas muscles

Variable	Value	Age	BMI	PDFF erector spinae muscles L3–L5	PDFF erector spinae muscles T12–L2	PDFF erector spinae muscles T9–T11	PDFF psoas muscles
Age	r	1.000	0.299	0.516	0.665	0.556	0.549
	P	–	0.009#	<0.001*	<0.001*	<0.001*	<0.001*
BMI	r	0.299	1.000	0.080	0.460	0.491	0.337
	P	0.009#	–	>0.05	<0.001*	<0.001*	0.003*
PDFF erector spinae muscles L3–L5	r	0.516	0.080	1.000	0.694	0.495	0.746
	P	<0.001*	>0.05	–	<0.001*	<0.001*	<0.001*
PDFF erector spinae muscles T12–L2	r	0.665	0.460	0.694	1.000	0.808	0.784
	P	<0.001*	<0.001*	<0.001*	–	<0.001*	<0.001*
PDFF erector spinae muscles T9–T11	r	0.556	0.491	0.495	0.808	1.000	0.643
	P	<0.001*	<0.001*	<0.001*	<0.001*	–	<0.001*
PDFF psoas muscles	r	0.549	0.337	0.746	0.784	0.643	1.000
	P	<0.001*	0.003*	<0.001*	<0.001*	<0.001*	–

*, statistically significant P values after Bonferroni correction for multiple testing (P<0.004). #, P values <0.05.

coefficient of variation in percent (relative units) amounted to 5.6% for the PDFF of the erector spinae muscles of the segment L3–L5, 6.2% for the segment T12–L2, 5.9% for the segment T9–T11, and 6.0% for the psoas muscles, respectively.

Discussion

The present investigation used chemical shift encoding-based water-fat MRI to extract the PDFF and CSA of the psoas muscles and three segments of the erector spinae

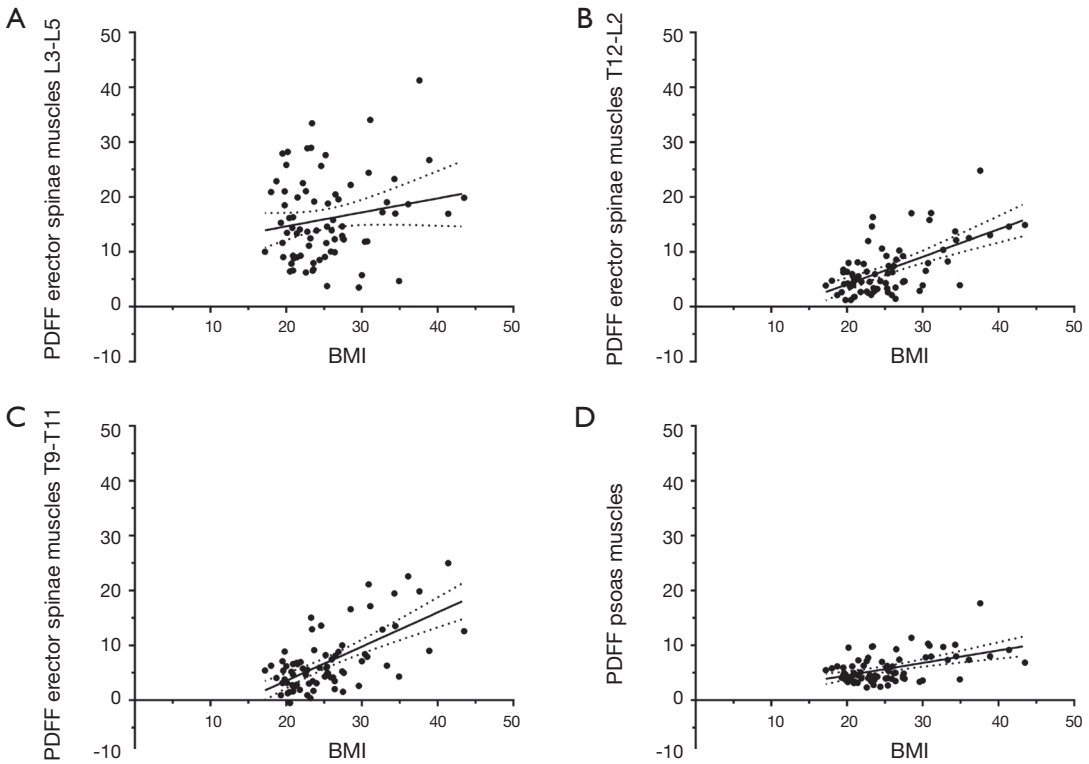

Figure 3 Body mass index (BMI) versus proton density fat fraction (PDFF). Graphs plotting the BMI (in kg/m^2, x-axis) against the PDFF (in %, y-axis) for the erector spinae muscles of the segments L3–L5 (A), T12–L2 (B), and T9–T11 (C) as well as the psoas muscles (D). Points represent the respective values of the single subjects, which are shown together with the best-fit line and its 95% confidence band.

Table 4 Partial correlation analyses in males between the proton density fat fraction (PDFF) of the erector spinae muscles of the segments L3–L5, T12–L2, and T9–T11, and the PDFF of psoas muscles. Age and body mass index (BMI) were included as control variables

Variable	Value	PDFF erector spinae muscles L3–L5	PDFF erector spinae muscles T12–L2	PDFF erector spinae muscles T9–T11	PDFF psoas muscles
PDFF erector spinae muscles L3–L5	r	1.000	0.923	0.502	0.819
	P	–	<0.001*	0.020#	<0.001*
PDFF erector spinae muscles T12–L2	r	0.923	1.000	0.673	0.847
	P	<0.001*	–	0.001*	<0.001*
PDFF erector spinae muscles T9–T11	r	0.502	0.673	1.000	0.373
	P	0.020#	0.001*	–	>0.05
PDFF psoas muscles	r	0.819	0.847	0.373	1.000
	P	<0.001*	<0.001*	>0.05	–

*, statistically significant P values after Bonferroni correction for multiple testing (P<0.008). #, P values <0.05.

Table 5 Partial correlation analyses in females between the proton density fat fraction (PDFF) of the erector spinae muscles of the segments L3–L5, T12–L2, and T9–T11, and the PDFF of psoas muscles. Age and body mass index (BMI) were included as control variables

Variable	Value	PDFF erector spinae muscles L3–L5	PDFF erector spinae muscles T12–L2	PDFF erector spinae muscles T9–T11	PDFF psoas muscles
PDFF erector spinae muscles L3–L5	r	1.000	0.547	0.316	0.386
	P	–	<0.001*	0.026#	0.006*
PDFF erector spinae muscles T12–L2	r	0.547	1.000	0.727	0.575
	P	<0.001*	–	<0.001*	<0.001*
PDFF erector spinae muscles T9–T11	r	0.316	0.727	1.000	0.495
	P	0.026#	<0.001*	–	<0.001*
PDFF psoas muscles	r	0.386	0.575	0.495	1.000
	P	0.006*	<0.001*	<0.001*	–

*, statistically significant P values after Bonferroni correction for multiple testing (P<0.008). #, P values <0.05.

muscles. The PDFF of the erector spinae muscles of the segment L3–L5 was independent of BMI and showed higher values when compared to the other segments. For the psoas muscles and the erector spinae muscles of the segment L3–L5, significant gender differences in PDFF values were observed. When considering age and BMI as control variables, significant correlations between segments of the erector spinae muscles were maintained for the PDFF in both genders.

Regarding measurements of the CSA of both the psoas muscles as well as the three segments of the erector spinae muscles, males showed significantly higher values when compared to their female counterparts. This finding is in accordance with previous studies, showing gender differences in CSA for the paraspinal musculature with clearly higher values for males (33,36). Accordingly, volumes of paraspinal muscles were also shown to be gender-specific, with larger volumes in males when compared to females (37). For the PDFF of the psoas muscles and the erector spinae muscles of the segment L3–L5 we found an inverse relationship, with males showing significantly lower values. This observation is again in concordance with previous studies investigating fat fractions by PDFF or other measures for paraspinal musculature (33,36,37). Regarding absolute values, a previous study in 26 healthy subjects of both genders (age: 30±6 years, BMI: 27.0±2.7 kg/m^2) using six-echo chemical shift encoding-based water-fat separation with segmentations of paraspinal muscles between the upper endplate level of L2 and the lower endplate level of L5 reported on PDFF values of 8.9%±2.1% in males and 11.6%±2.9% in females for the erector spinae muscles and 4.9%±1.1% in males and 5.3%±1.8% in females for the psoas muscles (36). Another study in females revealed PDFF values of 11.6±2.9% in premenopausal women (age: 29.9±7.1 years, BMI: 26.0±1.6 kg/m^2) and 24.6%±7.1% in postmenopausal women (age: 63.2±6.3 years, BMI: 25.7±4.2 kg/m^2) for erector spinae muscles, also derived from chemical shift encoding-based water-fat MRI with six echoes and the same method and area of muscle segmentation (34). The PDFF values extracted in this study seem to be principally in agreement with published data, with discrepancies being most likely attributable to differences in subject characteristics such as age, BMI, hormonal status, or gender distributions. In this context, it has already been shown by MRI-based investigations that fat fractions are subject to considerable variation even in the absence of any disease, thus depending on demographic characteristics and the effect of aging (37-40). Moreover, fat fractions can show early and significant increases in the course of many pathologies, including metabolic, neuromuscular, degenerative and other diseases (7-16).

Concerning potential regional variation of fat fractions in the paraspinal musculature, there is scarce data. A previous study enrolled 40 healthy males (age: 40.0±11.2 years, BMI: 23.0±1.8 kg/m^2) and 40 healthy females (age: 39.0±11.6 years, BMI: 21.6±2.1 kg/m^2) and performed an evaluation of the fat fraction of the multifidus and erector spinae muscles at the levels L1–L5 as derived from two-echo DIXON imaging (37). The study showed an increase in fat fractions from L1 to L5, with fat fractions in L5 reaching the highest values in both genders (males: 25.7%±8.0%, females: 31.9%±9.3%) (37). We revealed the

highest PDFF values for the segment L3–L5 of erector spinae muscles (males: 10.7%±7.6%, females: 18.2%±6.8%), whereas the segments T12–L2 and T9–T11 showed clearly lower PDFF values. Although both studies report on the highest fat fractions for paraspinal musculature on the level of the lower instead of the middle or upper lumbar spine, considerable differences in absolute values seem evident. In this context, the previous study used only two echoes during imaging, potentially leading to aberrant fat quantifications when compared to imaging with higher echo numbers, such as six or eight echoes. Further, T1-bias and T2*-decay effects can lead to over- or underestimations of fat fractions (24,41,42). Against this background, the present study may provide more accurate estimations of fat fractions by means of PDFF using chemical shift encoding-based water-fat MRI with six echoes and a smaller flip angle to further reduce T1-bias effects. Furthermore, it expands the evidence for regional variations of fat fractions of paraspinal musculature by not only evaluating muscles on the lumbar level; instead, we also included lower thoracic levels up to T9. More importantly, we were able to show that the PDFF of the segment L3–L5 of the erector spinae muscles was independent of BMI.

The absence of an association of the BMI with the PDFF of the segment L3–L5 of the erector spinae muscles might potentially suggest that muscle segmentation of this level could be preferred over segmentation of the level T12–L2 or T9–T11 when segmentations should be restricted to a rather circumscribed area. This suggestion might at least hold true for healthy subjects as investigated in the present study. Patients that suffer from rather localized, focal pathologic conditions affecting muscle volume and fat fractions may show different patterns. Such conditions could be present in patients with vertebral fractures who have shown changes in paraspinal musculature (16,43); however, further evidence to make more distinct recommendations is needed. The need for identification of representative, independent levels for segmentation of paraspinal musculature is related to the commonly applied approaches of semi-automatic or manual segmentation, which have shown to be time consuming particularly when performed on several consecutive MRI slices instead of on one slice only (44,45). Thus, restrictions to the most suitable or representative areas are generally welcome, with the finding of the PDFF of the segment L3–L5 of the erector spinae muscles being independent of BMI providing a rationale for segmentations of a specific level when resources are limited. Furthermore, the PDFF of this muscle and level might qualify as a potential biomarker for muscle alterations due to the absence of significant associations with BMI, a factor commonly regarded as a confounder of absolute values of fat quantity.

However, there are shortcomings of this study that need to be considered. First, the cohort included more female subjects than males and, thus, was not equally balanced regarding gender distribution. Second, we did not explicitly include subjects with a diagnosis of metabolic, neuromuscular, degenerative or other diseases that have an impact on fat fractions of musculature (7-16). Third, to measure PDFF, this study used chemical shift encoding-based water-fat MRI only, which is a modern field map-insensitive technique enabling spatially resolved fat quantification, but it does not allow for the quantification of intramyocellular and extramyocellular lipid levels like MRS does (17-19,21). Taken together, future studies may include patients with defined diseases and should make advantage of a multi-modal setup combining chemical shift encoding-based water-fat MRI and MRS to also deliver insights into intramuscular lipid distributions. Additionally, such studies may allow to investigate further the potential role of the PDFF of the segment L3–L5 of the erector spinae muscles as a biomarker for muscle alterations.

In conclusion, the results derived from this study may offer new perspectives for a better understanding of basal muscle physiology. Of note, the PDFF of the erector spinae muscles at the level L3–L5 showed to be not dependent on BMI, suggesting that this level might be suitable for paraspinal muscle segmentations when time resources for manual segmentation of larger areas are restricted. However, future studies including patients with diseases entailing alterations in fat composition and distribution will have to investigate further the role of the PDFF of this level as a potential biomarker. Furthermore, distinct causes for the finding of higher PDFF values of paraspinal musculature at the segment L3–L5 when compared to segments above should be investigated.

Acknowledgments

Funding: This research was supported by the European Research Council (grant agreement No. 677661—ProFatMRI and grant agreement No. 637164—iBack), the German Research Foundation (DFG-SFB824/A9), Philips Healthcare, the Else Kroener-Fresenius-Foundation, the Helmholtz cross-program topic “Metabolic Dysfunction”, and the Technical University of Munich (TUM) in the

framework of the Open Access Publishing Program. This work reflects only the authors' view and the funding agencies are not responsible for any use that may be made of the information it contains.

Footnote

Conflicts of Interest: The authors have no conflicts of interest to declare.

Ethical Statement: This study was approved by the Institutional Review Board (registration number: 2719/10 S) and was conducted in accordance with the Declaration of Helsinki. Written informed consent was obtained from all study participants.

References

1. Popkin BM, Hawkes C. Sweetening of the global diet, particularly beverages: patterns, trends, and policy responses. Lancet Diabetes Endocrinol 2016;4:174-86.
2. Hill JO, Wyatt HR, Peters JC. Energy balance and obesity. Circulation 2012;126:126-32.
3. Hill JO. Understanding and addressing the epidemic of obesity: an energy balance perspective. Endocr Rev 2006;27:750-61.
4. Ibrahim MM. Subcutaneous and visceral adipose tissue: structural and functional differences. Obes Rev 2010;11:11-8.
5. Freedland ES. Role of a critical visceral adipose tissue threshold (CVATT) in metabolic syndrome: implications for controlling dietary carbohydrates: a review. Nutr Metab (Lond) 2004;1:12.
6. Wajchenberg BL. Subcutaneous and visceral adipose tissue: their relation to the metabolic syndrome. Endocr Rev 2000;21:697-738.
7. Karampinos DC, Baum T, Nardo L, Alizai H, Yu H, Carballido-Gamio J, Yap SP, Shimakawa A, Link TM, Majumdar S. Characterization of the regional distribution of skeletal muscle adipose tissue in type 2 diabetes using chemical shift-based water/fat separation. J Magn Reson Imaging 2012;35:899-907.
8. Kumar D, Karampinos DC, MacLeod TD, Lin W, Nardo L, Li X, Link TM, Majumdar S, Souza RB. Quadriceps intramuscular fat fraction rather than muscle size is associated with knee osteoarthritis. Osteoarthritis Cartilage 2014;22:226-34.
9. Teichtahl AJ, Urquhart DM, Wang Y, Wluka AE, Wijethilake P, O'Sullivan R, Cicuttini FM. Fat infiltration of paraspinal muscles is associated with low back pain, disability, and structural abnormalities in community-based adults. Spine J 2015;15:1593-601.
10. Urrutia J, Besa P, Lobos D, Campos M, Arrieta C, Andia M, Uribe S. Lumbar paraspinal muscle fat infiltration is independently associated with sex, age, and inter-vertebral disc degeneration in symptomatic patients. Skeletal Radiol 2018;47:955-61.
11. Shahidi B, Parra CL, Berry DB, Hubbard JC, Gombatto S, Zlomislic V, Allen RT, Hughes-Austin J, Garfin S, Ward SR. Contribution of Lumbar Spine Pathology and Age to Paraspinal Muscle Size and Fatty Infiltration. Spine (Phila Pa 1976) 2017;42:616-23.
12. Dahlqvist JR, Vissing CR, Thomsen C, Vissing J. Severe paraspinal muscle involvement in facioscapulohumeral muscular dystrophy. Neurology 2014;83:1178-83.
13. Elliott JM, Courtney DM, Rademaker A, Pinto D, Sterling MM, Parrish TB. The Rapid and Progressive Degeneration of the Cervical Multifidus in Whiplash: An MRI Study of Fatty Infiltration. Spine (Phila Pa 1976) 2015;40:E694-700.
14. Sun D, Liu P, Cheng J, Ma Z, Liu J, Qin T. Correlation between intervertebral disc degeneration, paraspinal muscle atrophy, and lumbar facet joints degeneration in patients with lumbar disc herniation. BMC Musculoskelet Disord 2017;18:167.
15. Janssen BH, Voet NB, Nabuurs CI, Kan HE, de Rooy JW, Geurts AC, Padberg GW, van Engelen BG, Heerschap A. Distinct disease phases in muscles of facioscapulohumeral dystrophy patients identified by MR detected fat infiltration. PLoS One 2014;9:e85416.
16. Kim JY, Chae SU, Kim GD, Cha MS. Changes of paraspinal muscles in postmenopausal osteoporotic spinal compression fractures: magnetic resonance imaging study. J Bone Metab 2013;20:75-81.
17. Baum T, Cordes C, Dieckmeyer M, Ruschke S, Franz D, Hauner H, Kirschke JS, Karampinos DC. MR-based assessment of body fat distribution and characteristics. Eur J Radiol 2016;85:1512-8.
18. Lemos T, Gallagher D. Current body composition measurement techniques. Curr Opin Endocrinol Diabetes Obes 2017;24:310-4.
19. Seabolt LA, Welch EB, Silver HJ. Imaging methods for analyzing body composition in human obesity and cardiometabolic disease. Ann N Y Acad Sci 2015;1353:41-59.
20. Petak S, Barbu CG, Yu EW, Fielding R, Mulligan K,

Sabowitz B, Wu CH, Shepherd JA. The Official Positions of the International Society for Clinical Densitometry: body composition analysis reporting. J Clin Densitom 2013;16:508-19.
21. Hu HH, Kan HE. Quantitative proton MR techniques for measuring fat. NMR Biomed 2013;26:1609-29.
22. Reeder SB, Hu HH, Sirlin CB. Proton density fat-fraction: a standardized MR-based biomarker of tissue fat concentration. J Magn Reson Imaging 2012;36:1011-4.
23. Hernando D, Liang ZP, Kellman P. Chemical shift-based water/fat separation: a comparison of signal models. Magn Reson Med 2010;64:811-22.
24. Karampinos DC, Yu H, Shimakawa A, Link TM, Majumdar S. T(1)-corrected fat quantification using chemical shift-based water/fat separation: application to skeletal muscle. Magn Reson Med 2011;66:1312-26.
25. Fischer MA, Nanz D, Shimakawa A, Schirmer T, Guggenberger R, Chhabra A, Carrino JA, Andreisek G. Quantification of muscle fat in patients with low back pain: comparison of multi-echo MR imaging with single-voxel MR spectroscopy. Radiology 2013;266:555-63.
26. Smith AC, Parrish TB, Abbott R, Hoggarth MA, Mendoza K, Chen YF, Elliott JM. Muscle-fat MRI: 1.5 Tesla and 3.0 Tesla versus histology. Muscle Nerve 2014;50:170-6.
27. Li G, Xu Z, Gu H, Li X, Yuan W, Chang S, Fan J, Calimente H, Hu J. Comparison of chemical shift-encoded water-fat MRI and MR spectroscopy in quantification of marrow fat in postmenopausal females. J Magn Reson Imaging 2017;45:66-73.
28. Shen W, Gong X, Weiss J, Jin Y. Comparison among T1-weighted magnetic resonance imaging, modified dixon method, and magnetic resonance spectroscopy in measuring bone marrow fat. J Obes 2013;2013:298675.
29. Ruschke S, Pokorney A, Baum T, Eggers H, Miller JH, Hu HH, Karampinos DC. Measurement of vertebral bone marrow proton density fat fraction in children using quantitative water-fat MRI. MAGMA 2017;30:449-60.
30. Hicks GE, Simonsick EM, Harris TB, Newman AB, Weiner DK, Nevitt MA, Tylavsky FA. Cross-sectional associations between trunk muscle composition, back pain, and physical function in the health, aging and body composition study. J Gerontol A Biol Sci Med Sci 2005;60:882-7.
31. Hansen L, de Zee M, Rasmussen J, Andersen TB, Wong C, Simonsen EB. Anatomy and biomechanics of the back muscles in the lumbar spine with reference to biomechanical modeling. Spine (Phila Pa 1976) 2006;31:1888-99.
32. Liu CY, McKenzie CA, Yu H, Brittain JH, Reeder SB. Fat quantification with IDEAL gradient echo imaging: correction of bias from T(1) and noise. Magn Reson Med 2007;58:354-64.
33. Burian E, Syvari J, Holzapfel C, Drabsch T, Kirschke JS, Rummeny EJ, Zimmer C, Hauner H, Karampinos DC, Baum T, Franz D. Gender- and Age-Related Changes in Trunk Muscle Composition Using Chemical Shift Encoding-Based Water-Fat MRI. Nutrients 2018. doi: 10.3390/nu10121972.
34. Sollmann N, Dieckmeyer M, Schlaeger S, Rohrmeier A, Syvaeri J, Diefenbach MN, Weidlich D, Ruschke S, Klupp E, Franz D, Rummeny EJ, Zimmer C, Kirschke JS, Karampinos DC, Baum T. Associations Between Lumbar Vertebral Bone Marrow and Paraspinal Muscle Fat Compositions-An Investigation by Chemical Shift Encoding-Based Water-Fat MRI. Front Endocrinol (Lausanne) 2018;9:563.
35. Gluer CC, Blake G, Lu Y, Blunt BA, Jergas M, Genant HK. Accurate assessment of precision errors: how to measure the reproducibility of bone densitometry techniques. Osteoporos Int 1995;5:262-70.
36. Schlaeger S, Inhuber S, Rohrmeier A, Dieckmeyer M, Freitag F, Klupp E, Weidlich D, Feuerriegel G, Kreuzpointner F, Schwirtz A, Rummeny EJ, Zimmer C, Kirschke JS, Karampinos DC, Baum T. Association of paraspinal muscle water-fat MRI-based measurements with isometric strength measurements. Eur Radiol 2019;29:599-608.
37. Crawford RJ, Filli L, Elliott JM, Nanz D, Fischer MA, Marcon M, Ulbrich EJ. Age- and Level-Dependence of Fatty Infiltration in Lumbar Paravertebral Muscles of Healthy Volunteers. AJNR Am J Neuroradiol 2016;37:742-8.
38. Roldan-Valadez E, Pina-Jimenez C, Favila R, Rios C. Gender and age groups interactions in the quantification of bone marrow fat content in lumbar spine using 3T MR spectroscopy: a multivariate analysis of covariance (Mancova). Eur J Radiol 2013;82:e697-702.
39. Kugel H, Jung C, Schulte O, Heindel W. Age- and sex-specific differences in the 1H-spectrum of vertebral bone marrow. J Magn Reson Imaging 2001;13:263-8.
40. Baum T, Rohrmeier A, Syvari J, Diefenbach MN, Franz D, Dieckmeyer M, Scharr A, Hauner H, Ruschke S, Kirschke JS, Karampinos DC. Anatomical Variation of Age-Related Changes in Vertebral Bone Marrow Composition Using Chemical Shift Encoding-Based Water-Fat Magnetic Resonance Imaging. Front Endocrinol (Lausanne)

2018;9:141.
41. Yu H, Shimakawa A, McKenzie CA, Brodsky E, Brittain JH, Reeder SB. Multiecho water-fat separation and simultaneous R2* estimation with multifrequency fat spectrum modeling. Magn Reson Med 2008;60:1122-34.
42. Loughran T, Higgins DM, McCallum M, Coombs A, Straub V, Hollingsworth KG. Improving highly accelerated fat fraction measurements for clinical trials in muscular dystrophy: origin and quantitative effect of R2* changes. Radiology 2015;275:570-8.
43. Huang CWC, Tseng IJ, Yang SW, Lin YK, Chan WP. Lumbar muscle volume in postmenopausal women with osteoporotic compression fractures: quantitative measurement using MRI. Eur Radiol 2019;29:4999-5006.
44. Antony J, McGuinness K, Welch N, Coyle J, Franklyn-Miller A, O'Connor NE, Moran K. An interactive segmentation tool for quantifying fat in lumbar muscles using axial lumbar-spine MRI. IRBM 2016;31:11-22.
45. Crawford RJ, Cornwall J, Abbott R, Elliott JM. Manually defining regions of interest when quantifying paravertebral muscles fatty infiltration from axial magnetic resonance imaging: a proposed method for the lumbar spine with anatomical cross-reference. BMC Musculoskelet Disord 2017;18:25.

Cite this article as: Sollmann N, Zoffl A, Franz D, Syväri J, Dieckmeyer M, Burian E, Klupp E, Hedderich DM, Holzapfel C, Drabsch T, Kirschke JS, Rummeny EJ, Zimmer C, Hauner H, Karampinos DC, Baum T. Regional variation in paraspinal muscle composition using chemical shift encoding-based water-fat MRI. Quant Imaging Med Surg 2020;10(2):496-507. doi: 10.21037/qims.2020.01.10

